



Evaluated kinetic and photochemical data for atmospheric chemistry: Volume IX – gas-phase reactions of halogenated alkanes, alkenes, and oxygenated compounds

Timothy J. Wallington¹, Markus Ammann², John N. Crowley³, Hartmut Herrmann⁴, Michael E. Jenkin⁵, V. Faye McNeill⁶, Abdelwahid Mellouki⁷, and Jürgen Troe^{8,9}

¹Center for Sustainable Systems, School for Environment and Sustainability, University of Michigan, Ann Arbor, Michigan 48109, USA

²PSI Center for Energy and Environmental Science, Paul Scherrer Institut, Forschungsstrasse 111, 5232 Villigen, Switzerland

³Max Planck Institute for Chemistry, Division of Atmospheric Chemistry, 55128 Mainz, Germany

⁴Atmospheric Chemistry Department (ACD), Leibniz Institute for Tropospheric Research (TROPOS), 04318 Leipzig, Germany

⁵Atmospheric Chemistry Services, Okehampton, Devon, EX20 4QB, UK

⁶Departments of Chemical Engineering and Earth and Environmental Sciences, Columbia University, New York, NY 10027, USA

⁷African Research Center on Air Quality and Climate (ARC Air), University Mohammed VI Polytechnic University (UM6P), Lot 660, Hay Moulay Rachid Ben Guerir, 43150, Morocco

⁸Georg-August-Universität, Institut für Physikalische Chemie, Tammannstraße 6, 37077 Göttingen, Germany

⁹Max Planck Institute for Multidisciplinary Sciences, Am Fassberg 11, 37077 Göttingen, Germany

Correspondence: Timothy J. Wallington (twalling@umich.edu) and John N. Crowley (john.crowley@mpic.de)

Received: 16 January 2026 – Discussion started: 29 January 2026

Revised: 6 April 2026 – Accepted: 8 April 2026 – Published: 18 May 2026

Abstract. This article, the ninth in the series, presents kinetic and photochemical data sheets evaluated by the International Union of Pure and Applied Chemistry (IUPAC) Task Group on Atmospheric Chemical Kinetic Data Evaluation. It covers an extension of the gas phase and photochemical reactions of halogenated alkanes, alkenes, and oxygenated organic compounds implemented on the IUPAC website since 2008. The article consists of a summary table of the recommended kinetic parameters for the evaluated reactions, and a supplement containing the data sheets providing information upon which the recommendations are made.

1 Introduction

In the mid-1970s it was appreciated that there was a need to establish an international panel to produce a set of critically evaluated rate parameters for reactions of interest for atmospheric chemistry. To this end the CODATA Task Group on Chemical Kinetics, under the auspices of the International Council of Scientific Unions (ICSU), was constituted

in 1977, and tasked to produce an evaluation of relevant, available kinetic and photochemical data. The first evaluation by this international committee was published in *J. Phys. Chem. Ref. Data* in 1980 (Baulch et al., 1980) and was followed by supplements in 1982 (Baulch et al., 1982) and 1984 (Baulch et al., 1984). In 1986 the IUPAC Subcommittee on Gas Kinetic Data Evaluation for Atmospheric Chemistry superseded the original CODATA Task Group for Atmospheric

Chemistry. The Subcommittee continued its data evaluation program with supplements published in 1989 (Atkinson et al., 1989), 1992 (Atkinson et al., 1992), 1997 (Atkinson et al., 1997a, b), 1999 (Atkinson et al., 1999), and 2000 (Atkinson et al., 2000).

Starting in 2005, the gas phase evaluation work was expanded to include heterogeneous reactions of gases on solid (Crowley et al., 2010) and liquid substrates (Ammann et al., 2013). Aqueous-phase reactions of atmospheric importance were added starting in 2015. The IUPAC group's work now includes over 1400 gas-phase, heterogeneous, and aqueous-phase reactions of importance in atmospheric chemistry. Reflecting the broader scope, the group changed its name to the IUPAC Task Group on Atmospheric Chemical Kinetic Data Evaluation in 2013. The history of IUPAC data evaluations and their role in addressing the critical societal challenges of stratospheric ozone loss, tropospheric ozone formation, acid rain, urban air pollution, aerosol formation, and climate change is discussed by Cox et al. (2018).

In 2000 the evaluation was made available on the worldwide web (<https://iupac.aeris-data.fr/>, last access: 29 April 2026). The IUPAC website hosts an interactive data base with a search facility and hyperlinks between the summary table and data sheets which can be downloaded as individual PDF files. Work is underway to provide machine readable metadata from the data sheets to enable automatic transfer of IUPAC recommended data into atmospheric models. The IUPAC group continues to update and extend the set of evaluated reactions. To enhance the accessibility of this updated material to the scientific community, the evaluation is being published as a series of articles in *Atmospheric Chemistry and Physics* (Atkinson et al., 2004, 2006, 2007, 2008; Crowley et al., 2010; Ammann et al., 2013; Cox et al., 2020; Mellouki et al., 2021).

The fourth article in this series covering small ($\leq C_3$) organic halogen species was published in 2008 (Atkinson et al., 2008). The past two decades have seen increasing concern regarding the presence of long-chain persistent bioaccumulative fluorinated organic pollutants such as perfluorooctanoic acid ($C_7F_{15}C(O)OH$, PFOA), perfluorooctane sulfonic acid ($C_8F_{17}S(O)OH$, PFOS), and per- and polyfluoroalkyl substances (PFAS) in the environment (Giesy and Kannan, 2001; Ellis et al., 2004; Lau et al., 2007; Prevedouros et al., 2006). Concern over the growing contribution of hydrofluorocarbons (HFCs) to radiative forcing of climate change (Velders et al., 2009) led to the recent Kigali Agreement to limit HFC emissions. Halogenated alkenes and oxygenates have been developed to replace HFCs (Brown, 2009; Burkholder et al., 2015; Wallington et al., 2015) and are used as industrial solvents, synthesis reagents for surface coatings, inhalation agents, fire retardants, fire-fighting foams, and surfactants (Wallington et al., 2017). To provide data relevant to understanding these new issues we have extended the set of evaluated reactions. Volume IX contains data sheets for gas-phase and photochemical reactions of halogenated organic

species added since publication of Volume IV (Atkinson et al., 2008).

2 Guide to the datasheets

For each reaction covered in this volume, a datasheet with details about e.g. experimental methods and a justification of the choice of preferred value is available in the supplementary information. The datasheets covering gas-phase reactions are principally of two types: (i) those for individual thermal reactions and (ii) those for the individual photochemical reactions. Rate coefficients are also known as rate constants, both terms are used here. The recommended kinetic parameters for the evaluated reactions are given in Table 1.

2.1 Thermal reactions

The datasheets begin with a statement of the reactions including all pathways which are considered feasible. The available kinetic data on the reactions are summarized under two headings: (i) Absolute Rate Coefficients, and (ii) Relative Rate Coefficients. Under these headings, we list the published experimental data as absolute rate coefficients. If the temperature dependence of the rate coefficient has been measured, the results are given in the temperature dependent form as stated by the authors over a stated temperature range. For bimolecular reactions, the temperature dependence is usually expressed in the conventional Arrhenius form, $k = A \exp(-B/T)$, where $B = E/R$. For a few bimolecular reactions, we have listed temperature dependences in alternative forms such as $k = C(T/298K)^n \exp(-D/T)$ or $k = ET^2 \exp(-F/T) \text{ cm}^3 \text{ molec.}^{-1} \text{ s}^{-1}$ where the original authors have found that alternative expressions give a better fit to the data. In our recommendations we seek to provide simple Arrhenius expressions that describe the kinetics over the atmospherically relevant temperature range (180–310 K). More complex expressions, which are often needed to describe the kinetic behaviour over larger ranges of temperature, are given in the Comments on Preferred Values section in the data sheets. Rate coefficients are given here in units of $\text{cm}^3 \text{ molec.}^{-1} \text{ s}^{-1}$. Note that “molecule” is not a unit, but is included for clarity. For pressure dependent combination and dissociation reactions, the non-Arrhenius temperature dependence is used. This is discussed more fully in Sect. 2.3 of this guide. Single-temperature data are presented as such and, wherever possible, the rate coefficient at, or close to, 298 K as measured by the original authors is quoted directly. This means that the listed rate coefficient at 298 K may differ slightly from that calculated from the Arrhenius parameters determined by the same authors. Rate coefficients at 298 K marked with an asterisk indicate that the value was calculated by extrapolation of a measured temperature range, which did not include 298 K. The tables of data are supplemented by a series of comments summarizing the experimental details. The abbreviations, relating to experimental techniques, used

Table 1. Summary of recommended rate coefficients^a for organic halogen reactions added since publication of Volume IV.

| Datasheet ID ^b | Reaction | $k_{298}/\text{cm}^3 \text{ molec.}^{-1} \text{ s}^{-1}$ | $\Delta \log k_{298}^c$ | $k(T)/\text{cm}^3 \text{ molec.}^{-1} \text{ s}^{-1}$ | Temp. range/K | $\Delta(E/R)/\text{K}^c$ |
|--|--|--|-------------------------|---|---------------|--------------------------|
| <i>Organic FO_x, ClO_x, BrO_x, and IO_x reactions added to the IUPAC website (see Supplement for datasheets)</i> | | | | | | |
| <i>Halogenated alkanes</i> | | | | | | |
| oFOX72 | HO + CF ₃ CH ₂ CH ₃ (HFC-263fb) → products | 4.9×10^{-14} | 0.15 | $3.7 \times 10^{-12} \exp(-1290/T)$ | 240–370 | 300 |
| oFOX73 | HO + CF ₃ CHFCH ₂ F (HFC-245eb) → products | 1.6×10^{-14} | 0.15 | $1.1 \times 10^{-11} \exp(-1250/T)$ | 240–380 | 300 |
| oFOX74 | HO + CHF ₂ CHFCHF ₂ (HFC-245ea) → products | 1.8×10^{-14} | 0.15 | $1.8 \times 10^{-12} \exp(-1375/T)$ | 240–380 | 300 |
| oFOX75 | HO + CF ₃ CH ₂ CHF ₂ (HFC-245fa) → products | 6.9×10^{-15} | 0.12 | $6.0 \times 10^{-13} \exp(-1331/T)$ | 270–370 | 300 |
| oFOX76 | HO + CF ₃ CH ₂ CF ₂ CH ₃ (HFC-365mfc) → products | 7.1×10^{-15} | 0.20 | $1.6 \times 10^{-12} \exp(-1620/T)$ | 270–380 | 200 |
| oFOX77 | HO + CF ₃ CH ₂ CH ₂ CF ₃ (HFC-356mfh) → products | 7.8×10^{-15} | 0.10 | $2.6 \times 10^{-12} \exp(-1734/T)$ | 260–370 | 300 |
| oFOX78 | HO + CF ₃ CF ₂ CH ₂ CH ₂ F (HFC-356mcf) → products | 4.2×10^{-14} | 0.15 | $1.7 \times 10^{-12} \exp(-1108/T)$ | 250–370 | 300 |
| oFOX79 | HO + CHF ₂ CF ₂ CF ₂ CHF ₂ (HFC-338pcc) → products | 4.3×10^{-15} | 0.08 | $7.82 \times 10^{-13} \exp(-1548/T)$ | 230–420 | 200 |
| oFOX80 | HO + CF ₃ CH ₂ CF ₂ CH ₂ CF ₃ (HFC-458mfef) → products | 2.6×10^{-15} | 0.15 | $1.23 \times 10^{-12} \exp(-1833/T)$ | 270–360 | 300 |
| oFOX81 | HO + CF ₃ CHFCHF ₂ CF ₃ (HFC-4410mee) → products | 3.3×10^{-15} | 0.12 | $5.68 \times 10^{-13} \exp(-1534/T)$ | 240–400 | 300 |
| oFOX82 | HO + CF ₃ CF ₂ CH ₂ CH ₂ CF ₂ CF ₃ (HFC-5510mcfh) → products | 8.3×10^{-15} | 0.20 | | | |
| oFOX83 | HO + CHF ₂ (CF ₂) ₄ CF ₃ (HFC-5213p) → products | 1.8×10^{-15} | 0.10 | $5.76 \times 10^{-13} \exp(-1726/T)$ | 250–430 | 300 |
| oClOX86 | HO + C ₂ H ₅ Cl → products | 3.7×10^{-13} | 0.10 | $4.25 \times 10^{-12} \exp(-727/T)$ | 220–400 | 200 |
| oClOX87 | HO + CH ₂ ClCH ₂ Cl → products | 2.4×10^{-13} | 0.08 | $8.69 \times 10^{-12} \exp(-1070/T)$ | 290–360 | 200 |
| oClOX88 | HO + CH ₃ CHCl ₂ → products | 2.76×10^{-13} | 0.10 | $2.04 \times 10^{-12} \exp(-596/T)$ | 290–370 | 300 |
| oBrOX16 | HO + CHBr ₃ → products | 2.7×10^{-13} | 0.15 | $1.00 \times 10^{-12} \exp(-388/T)$ | 290–370 | 300 |
| oBrOX17 | HO + C ₂ H ₅ Br → products | 3.3×10^{-13} | 0.15 | $2.25 \times 10^{-12} \exp(-576/T)$ | 230–300 | 300 |
| oBrOX18 | HO + CH ₂ BrCH ₂ Br → products | 2.22×10^{-13} | 0.10 | $7.69 \times 10^{-12} \exp(-1056/T)$ | 290–370 | 300 |
| oBrOX19 | HO + <i>n</i> -C ₃ H ₇ Br → products | 1.0×10^{-12} | 0.10 | $3.91 \times 10^{-12} \exp(-399/T)$ | 210–300 | 300 |
| oBrOX20 | HO + CH ₃ CHBrCH ₃ → products | 7.58×10^{-13} | 0.06 | $1.96 \times 10^{-12} \exp(-283/T)$ | 210–355 | 200 |
| oBrOX21 | HO + <i>n</i> -C ₄ H ₉ Br → products | 2.3×10^{-12} | 0.20 | | | |
| oBrOX22 | HO + <i>n</i> -C ₅ H ₁₁ Br → products | 3.7×10^{-12} | 0.20 | | | |
| oBrOX23 | HO + <i>n</i> -C ₆ H ₁₃ Br → products | 5.5×10^{-12} | 0.20 | | | |
| oIOx4 | HO + CH ₃ CH ₂ I → products | 3.43×10^{-13} | 0.10 | $5.55 \times 10^{-12} \exp(-830/T)$ | 290–380 | 200 |
| oIOx5 | HO + CH ₃ CH ₂ CH ₂ I → products | 1.36×10^{-12} | 0.08 | $1.86 \times 10^{-11} \exp(-780/T)$ | 290–380 | 200 |
| oIOx6 | HO + CH ₃ CHICH ₃ → products | 1.29×10^{-12} | 0.08 | $7.64 \times 10^{-11} \exp(-530/T)$ | 290–380 | 200 |
| oFOX108 | Cl + CHF ₂ CH ₂ CF ₃ (HFC-245fa) → products | 6.9×10^{-15} | 0.30 | | | |
| oFOX110 | Cl + CF ₃ CHF ₂ CF ₃ (HFC-227ea) → products | 4.4×10^{-16} | 0.15 | | | |
| oFOX111 | Cl + CHF ₃ (HFC-23) → products | 3.4×10^{-18} | 0.50 | | | |

Table 1. Continued.

| Dataseet ID ^b | Reaction | k_{298}^a cm ³ molec. ⁻¹ s ⁻¹ | $\Delta \log k_{298}^a$ | $k(T)^a$ cm ³ molec. ⁻¹ s ⁻¹ | Temp. range/K | $\Delta(E_a/R)^a$ K ^c |
|----------------------------|--|---|-------------------------|--|------------------|-------------------------------------|
| oBoOx24 | Cl + CH ₃ Br → products | 4.5×10^{-13} | 0.05 | $1.38 \times 10^{-11} \exp(-1020/T)$ | 210–300 | 100 |
| <i>Halogenated alkenes</i> | | | | | | |
| oFOx112 | HO + CF ₂ =CF ₂ (HFO-1114) → products | 1.04×10^{-11} | 0.06 | $3.84 \times 10^{-12} \exp(297/T)$ | 250–500 | 100 |
| oFOx114 | HO + CF ₃ CF=CH ₂ (HFO-1234yf) → products | 1.12×10^{-11} | 0.06 | $1.16 \times 10^{-12} \exp(-10/T)$ | 200–300 | 100 |
| oFOx115 | HO + <i>E</i> -CF ₃ CH=CHF (HFO-1234ze(<i>E</i>)) → products | 7.07×10^{-13} | 0.06 | $6.91 \times 10^{-13} \exp(7/T)$ | 210–300 | 100 |
| oFOx117 | HO + <i>Z</i> -CF ₃ CH=CHF (HFO-1234ze(<i>Z</i>)) → products | 1.21×10^{-12} | 0.15 | $8.46 \times 10^{-13} \exp(106/T)$ | 260–300 | 100 |
| oFOx118 | HO + <i>E</i> -CF ₃ CF=CHF (HFO-1225ze(<i>E</i>)) → products | 2.2×10^{-12} | 0.15 | | | |
| oFOx119 | HO + <i>Z</i> -CF ₃ CF=CHF (HFO-1225ze(<i>Z</i>)) → products | 1.2×10^{-12} | 0.10 | $7.60 \times 10^{-13} \exp(155/T)$ | 200–300 | 100 |
| oFOx116 | HO + CF ₃ CF ₂ =CF ₂ (FO-1216) → products | 2.18×10^{-12} | 0.04 | $7.38 \times 10^{-13} \exp(322/T)$ | 240–340 | 100 |
| oFOx135 | HO + <i>E</i> -CF ₃ CH=CHCF ₃ (HFO-1336mzz(<i>E</i>)) → products | 1.31×10^{-13} | 0.06 | $6.94 \times 10^{-13} \exp(-496/T)$ | 210–380 | 100 |
| oFOx136 | HO + <i>Z</i> -CF ₃ CH=CHCF ₃ (HFO-1336mzz(<i>Z</i>)) → products | 4.80×10^{-13} | 0.06 | $2.46 \times 10^{-13} \exp(199/T)$ | 210–300 | 100 |
| oClOx95 | HO + CH ₂ =CHCl (vinyl chloride) → products | 7.55×10^{-12} | 0.08 | $2.54 \times 10^{-12} \exp(325/T)$ | 280–600 | 100 |
| oFOx120 | HO + <i>E</i> -CF ₃ CH=CHCl (HCFPO-1233zd(<i>E</i>)) → products | 3.53×10^{-13} | 0.06 | $8.79 \times 10^{-13} \exp(-272/T)$ | 220–300 | 100 |
| oFOx121 | HO + <i>Z</i> -CF ₃ CH=CHCl (HCFPO-1233zd(<i>Z</i>)) → products | 9.24×10^{-13} | 0.06 | $3.61 \times 10^{-13} \exp(280/T)$ | 220–300 | 100 |
| oFOx165 | HO + <i>E</i> -CF ₃ CF=CHCl (HCFO-1224yd(<i>E</i>)) → products | 1.30×10^{-12} | 0.08 | $1.09 \times 10^{-12} \exp(53/T)$ | 250–430 | 100 |
| oFOx166 | HO + <i>Z</i> -CF ₃ CF=CHCl (HCFO-1224yd(<i>Z</i>)) → products | 5.83×10^{-13} | 0.08 | $8.03 \times 10^{-13} \exp(-95/T)$ | 250–430 | 100 |
| oFOx164 | HO + <i>E</i> -CF ₃ CBr=CH ₂ (HBFO-1233x(B)) → products | 3.84×10^{-12} | 0.06 | $1.11 \times 10^{-12} \exp(370/T)$ | 250–430 | 100 |
| oFOx154 | NO ₃ + CF ₂ =CF ₂ (HFO-1114) → products | $< 3 \times 10^{-15}$ | | | | |
| oFOx153 | NO ₃ + CF ₃ CF ₂ =CH ₂ (HFO-1234yf) → products | 2.6×10^{-17} | 0.15 | | | |
| oFOx122 | NO ₃ + <i>Z</i> -CF ₃ CF=CHF (HFO-1225ye(<i>Z</i>)) → products | 4.2×10^{-18} | 0.20 | | | |
| oFOx123 | NO ₃ + CF ₃ CF ₂ =CF ₂ (FO-1216) → products | $< 3 \times 10^{-15}$ | | | | |
| oFOx155 | NO ₃ + CF ₂ =CFCF=CF ₂ → products | 1.56×10^{-15} | 0.15 | | | |
| oClOx96 | NO ₃ + CH ₂ =CHCl (vinyl chloride) → products | 4.6×10^{-16} | 0.10 | $1.8 \times 10^{-13} \exp(-1780/T)$ | 260–380 | 300 |
| oFOx126 | O ₃ + CF ₂ =CF ₂ (HFO-1114) → products | 4.8×10^{-21} | 0.15 | | | |
| oFOx113 | O ₃ + CF ₃ CH=CH ₂ (HFO-1243zf) → products | 1.43×10^{-20} | 0.08 | $4.65 \times 10^{-16} \exp(-3096/T)$ | 290–390 | 200 |
| oFOx128 | O ₃ + CF ₃ CF=CH ₂ (HFO-1234yf) → products | 2.67×10^{-21} | 0.08 | | | |
| oFOx129 | O ₃ + <i>E</i> -CF ₃ CH=CHF (HFO-1234ze(<i>E</i>)) → products | 2.50×10^{-21} | 0.10 | | | |
| oFOx156 | O ₃ + <i>Z</i> -CF ₃ CH=CHF (HFO-1234ze(<i>Z</i>)) → products | 1.7×10^{-21} | 0.30 | | | |
| oFOx130 | O ₃ + CF ₃ CF ₂ =CF ₂ (FO-1216) → products | 6.2×10^{-22} | 0.15 | | | |
| oFOx157 | O ₃ + CF ₂ =CFCF=CF ₂ → products | 7.9×10^{-21} | 0.20 | $9.51 \times 10^{-17} \exp(-2800/T)$ | 220–320 | 200 |
| oFOx127 | O ₃ + <i>E</i> -CF ₃ CH=CHCF ₃ (HFO-1336mzz(<i>E</i>)) → products | 4.14×10^{-22} | 0.10 | | | |
| oFOx124 | O ₃ + <i>Z</i> -CF ₃ CH=CHCF ₃ (HFO-1336mzz(<i>Z</i>)) → products | 7.09×10^{-22} | 0.08 | | | |

Table 1. Continued.

| Datasheet ID ^b | Reaction | $k_{298}/\text{cm}^3 \text{ molec.}^{-1} \text{ s}^{-1}$ | $\Delta \log k_{298}^a/c$ | $k(T)/\text{cm}^3 \text{ molec.}^{-1} \text{ s}^{-1}$ | Temp. range/K | $\Delta(E/R)/\text{K}^c$ |
|------------------------------|---|--|---------------------------|---|---------------|--------------------------|
| oClOx97 | $\text{O}_3 + \text{CH}_2=\text{CHCl}$ (vinyl chloride) \rightarrow products | 2.5×10^{-19} | 0.20 | | | |
| oFox132 | $\text{O}_3 + E\text{-CF}_3\text{CH}=\text{CHCl}$ (HCFO-1233zd(E)) \rightarrow products | 1.51×10^{-21} | 0.15 | | | |
| oFox131 | $\text{O}_3 + Z\text{-CF}_3\text{CH}=\text{CHCl}$ (HCFO-1233zd(Z)) \rightarrow products | 1.53×10^{-21} | 0.15 | | | |
| oFox125 | $\text{O}_3 + \text{CF}_3\text{CCl}=\text{CH}_2$ (HCFO-1233xf) \rightarrow products | 3.00×10^{-21} | 0.08 | | | |
| <i>Halogenated alcohols</i> | | | | | | |
| oFox84 | $\text{HO} + \text{CH}_2\text{FCH}_2\text{OH} \rightarrow$ products | 9.12×10^{-13} | 0.08 | $2.23 \times 10^{-12} \exp(-266/T)$ | 230–300 | 100 |
| oFox85 | $\text{HO} + \text{CHF}_2\text{CH}_2\text{OH} \rightarrow$ products | 2.61×10^{-13} | 0.08 | $1.63 \times 10^{-12} \exp(-545/T)$ | 220–300 | 200 |
| oFox86 | $\text{HO} + \text{CF}_3\text{CH}_2\text{OH} \rightarrow$ products | 1.00×10^{-13} | 0.06 | $1.25 \times 10^{-12} \exp(-754/T)$ | 220–300 | 100 |
| oFox87 | $\text{HO} + \text{CF}_3\text{CH}_2\text{CH}_2\text{OH} \rightarrow$ products | 9.6×10^{-13} | 0.10 | $2.72 \times 10^{-12} \exp(-305/T)$ | 260–360 | 100 |
| oFox88 | $\text{HO} + \text{C}_2\text{F}_5\text{CH}_2\text{OH} \rightarrow$ products | 1.05×10^{-13} | 0.06 | $1.28 \times 10^{-12} \exp(-748/T)$ | 250–430 | 200 |
| oFox89 | $\text{HO} + \text{CF}_3\text{CH}(\text{OH})\text{CF}_3 \rightarrow$ products | 2.43×10^{-14} | 0.12 | $3.94 \times 10^{-15} (T/298)^{4.57} \exp(542/T)$ | 220–430 | |
| oFox158 | $\text{HO} + (\text{CF}_3)_2\text{C}(\text{OH})\text{CH}_3 \rightarrow$ products | 7.71×10^{-15} | 0.12 | $1.90 \times 10^{-18} (T/298)^{11.5} \exp(2476/T)$ | 230–370 | |
| oFox159 | $\text{HO} + (\text{CF}_3)_3\text{COH} \rightarrow$ products | 8.6×10^{-16} | 0.12 | $3.0 \times 10^{-20} (T/298)^{11.3} \exp(3060/T)$ | 230–370 | |
| oFox90 | $\text{HO} + \text{CF}_3\text{CHF}_2\text{CH}_2\text{OH} \rightarrow$ products | 1.3×10^{-13} | 0.12 | $2.26 \times 10^{-12} \exp(-848/T)$ | 250–430 | 200 |
| oFox91 | $\text{HO} + n\text{-C}_3\text{F}_7\text{CH}_2\text{OH} \rightarrow$ products | 1.11×10^{-13} | 0.10 | $6.06 \times 10^{-12} \exp(-1192/T)$ | 280–370 | 200 |
| oFox92 | $\text{HO} + n\text{-C}_4\text{F}_9\text{CH}_2\text{OH} \rightarrow$ products | 9.4×10^{-14} | 0.15 | | | |
| oFox93 | $\text{HO} + n\text{-C}_4\text{F}_9\text{CH}_2\text{CH}_2\text{OH} \rightarrow$ products | 1.0×10^{-12} | 0.15 | | | |
| oFox94 | $\text{HO} + n\text{-C}_6\text{F}_{13}\text{CH}_2\text{CH}_2\text{OH} \rightarrow$ products | 8.3×10^{-13} | 0.15 | | | |
| oFox95 | $\text{HO} + n\text{-C}_8\text{F}_{17}\text{CH}_2\text{CH}_2\text{OH} \rightarrow$ products | 9.2×10^{-13} | 0.15 | | | |
| oFox96 | $\text{HO} + \text{CF}_3\text{CH}(\text{OH})_2 \rightarrow$ products | 1.2×10^{-13} | 0.20 | | | |
| oClOx90 | $\text{HO} + \text{CH}_2\text{ClCH}_2\text{OH} \rightarrow$ products | 1.3×10^{-12} | 0.20 | | | |
| oClOx91 | $\text{HO} + \text{CCl}_3\text{CH}_2\text{OH} \rightarrow$ products | 2.45×10^{-13} | 0.20 | | | |
| <i>Halogenated aldehydes</i> | | | | | | |
| oFox97 | $\text{HO} + \text{CHF}_2\text{CHO} \rightarrow$ products | 1.6×10^{-12} | 0.15 | | | |
| oFox98 | $\text{HO} + \text{C}_2\text{F}_5\text{CHO} \rightarrow$ products | 5.2×10^{-13} | 0.10 | $2.42 \times 10^{-12} \exp(-458/T)$ | 250–360 | 200 |
| oFox99 | $\text{HO} + n\text{-C}_3\text{F}_7\text{CHO} \rightarrow$ products | 5.8×10^{-13} | 0.08 | $2.0 \times 10^{-12} \exp(-369/T)$ | 250–380 | 200 |
| oFox100 | $\text{HO} + n\text{-C}_4\text{F}_9\text{CHO} \rightarrow$ products | 6.1×10^{-13} | 0.08 | $2.0 \times 10^{-12} \exp(-356/T)$ | 250–380 | 150 |
| oFox101 | $\text{HO} + \text{CF}_3\text{CH}_2\text{CHO} \rightarrow$ products | 2.7×10^{-12} | 0.15 | $7.74 \times 10^{-12} \exp(-314/T)$ | 260–360 | 150 |
| oFox102 | $\text{HO} + n\text{-C}_6\text{F}_{13}\text{CH}_2\text{CHO} \rightarrow$ products | 2.0×10^{-12} | 0.15 | | | |
| oFox103 | $\text{HO} + n\text{-C}_8\text{F}_{17}\text{CH}_2\text{CHO} \rightarrow$ products | 1.8×10^{-12} | 0.15 | | | |

Table 1. Continued.

| Dataset ID ^b | Reaction | $k_{298}/\text{cm}^3 \text{ molec.}^{-1} \text{ s}^{-1}$ | $\Delta \log k_{298}^a$ | $k(T)/\text{cm}^3 \text{ molec.}^{-1} \text{ s}^{-1}$ | Temp. range/K | $\Delta(E/R)/\text{K}^c$ |
|---------------------------------|--|--|-------------------------|---|---------------|--------------------------|
| <i>Halogenated ketones</i> | | | | | | |
| oFox104 | $\text{HO} + \text{C}_2\text{F}_5\text{C}(\text{O})\text{CF}(\text{CF}_3)_2 \rightarrow \text{products}$ | $< 5 \times 10^{-16}$ | | | | |
| oClOx92 | $\text{HO} + \text{CH}_2\text{ClC}(\text{O})\text{CH}_3 \rightarrow \text{products}$ | 4.4×10^{-13} | 0.15 | | | |
| oClOx93 | $\text{HO} + \text{CHCl}_2\text{C}(\text{O})\text{CH}_3 \rightarrow \text{products}$ | 4.0×10^{-13} | 0.15 | | | |
| oClOx94 | $\text{HO} + \text{CCl}_3\text{C}(\text{O})\text{CH}_3 \rightarrow \text{products}$ | 1.5×10^{-14} | 0.15 | | | |
| <i>Halogenated acids</i> | | | | | | |
| oFox105 | $\text{HO} + \text{C}_2\text{F}_5\text{C}(\text{O})\text{OH} \rightarrow \text{products}$ | 1.55×10^{-13} | 0.15 | | | |
| oFox106 | $\text{HO} + n\text{-C}_3\text{F}_7\text{C}(\text{O})\text{OH} \rightarrow \text{products}$ | 1.55×10^{-13} | 0.15 | | | |
| oFox107 | $\text{HO} + n\text{-C}_4\text{F}_9\text{C}(\text{O})\text{OH} \rightarrow \text{products}$ | 1.55×10^{-13} | 0.15 | | | |
| <i>Halogenated ethers</i> | | | | | | |
| oFox137 | $\text{HO} + \text{CH}_3\text{OCHF}_2 \rightarrow \text{products}$ | 3.52×10^{-14} | 0.15 | $1.16 \times 10^{-11} \exp(-1728/T)$ | 290–470 | 100 |
| oFox138 | $\text{HO} + \text{CH}_3\text{OCHF}_3 \rightarrow \text{products}$ | 1.29×10^{-14} | 0.10 | $1.10 \times 10^{-12} \exp(-1324/T)$ | 290–470 | 100 |
| oFox139 | $\text{HO} + \text{CHF}_2\text{OCHF}_2 \rightarrow \text{products}$ | 2.20×10^{-15} | 0.10 | $1.04 \times 10^{-12} \exp(-1836/T)$ | 270–470 | 100 |
| oFox140 | $\text{HO} + \text{CHF}_2\text{OCF}_3 \rightarrow \text{products}$ | 4.57×10^{-16} | 0.10 | $3.09 \times 10^{-13} \exp(-1942/T)$ | 290–400 | 100 |
| oFox141 | $\text{HO} + \text{CH}_3\text{OCHF}_2\text{CF}_3 \rightarrow \text{products}$ | 1.57×10^{-13} | 0.10 | $1.74 \times 10^{-12} \exp(-716/T)$ | 250–330 | 100 |
| oFox142 | $\text{HO} + \text{CH}_3\text{OCF}_2\text{CHF}_2 \rightarrow \text{products}$ | 2.24×10^{-14} | 0.10 | $2.50 \times 10^{-12} \exp(-1405/T)$ | 240–440 | 100 |
| oFox143 | $\text{HO} + \text{CH}_3\text{OCH}_2\text{CF}_3 \rightarrow \text{products}$ | 6.56×10^{-13} | 0.10 | $3.61 \times 10^{-12} \exp(-508/T)$ | 260–360 | 300 |
| oFox144 | $\text{HO} + \text{CH}_3\text{OC}_2\text{F}_5 \rightarrow \text{products}$ | 1.20×10^{-14} | 0.10 | $1.84 \times 10^{-12} \exp(-1499/T)$ | 240–440 | 100 |
| oFox145 | $\text{HO} + n\text{-C}_3\text{F}_7\text{OCH}_3 \rightarrow \text{products}$ | 1.18×10^{-14} | 0.10 | $1.98 \times 10^{-12} \exp(-1526/T)$ | 240–440 | 100 |
| oFox146 | $\text{HO} + i\text{-C}_3\text{F}_7\text{OCH}_3 \rightarrow \text{products}$ | 1.52×10^{-14} | 0.10 | $1.86 \times 10^{-12} \exp(-1432/T)$ | 240–440 | 100 |
| oFox147 | $\text{HO} + \text{C}_4\text{F}_9\text{OCH}_3 \rightarrow \text{products}$ | 1.19×10^{-14} | 0.08 | $1.15 \times 10^{-12} \exp(-1362/T)$ | 250–330 | 100 |
| oFox148 | $\text{HO} + \text{CH}_3\text{OCH}(\text{CF}_3)_2 \rightarrow \text{products}$ | 2.29×10^{-13} | 0.10 | $1.08 \times 10^{-12} \exp(-461/T)$ | 230–340 | 100 |
| oFox149 | $\text{HO} + \text{CH}_2\text{FOCH}(\text{CF}_3)_2 \text{ (Sevoflurane)} \rightarrow \text{products}$ | 4.10×10^{-14} | 0.10 | $1.24 \times 10^{-12} \exp(-1017/T)$ | 230–440 | 200 |
| oFox150 | $\text{HO} + \text{CHF}_2\text{OCHF}_2\text{CF}_3 \text{ (Desflurane)} \rightarrow \text{products}$ | 4.08×10^{-15} | 0.10 | $7.43 \times 10^{-13} \exp(-1551/T)$ | 230–300 | 200 |
| <i>Halogenated vinyl ethers</i> | | | | | | |
| oFox133 | $\text{HO} + \text{CF}_3\text{OCF}=\text{CF}_2 \rightarrow \text{products}$ | 2.96×10^{-12} | 0.10 | $1.01 \times 10^{-12} \exp(320/T)$ | 250–430 | 100 |
| oFox134 | $\text{HO} + \text{C}_2\text{F}_5\text{OCF}=\text{CF}_2 \rightarrow \text{products}$ | 3.0×10^{-12} | 0.10 | $6.0 \times 10^{-13} \exp(480/T)$ | 200–300 | 100 |

Table 1. Continued.

| Datasheet ID ^b | Reaction | $k_{298}/\text{cm}^3 \text{ molec.}^{-1} \text{ s}^{-1}$ | $\Delta \log k_{298}^a$ | $k(T)/\text{cm}^3 \text{ molec.}^{-1} \text{ s}^{-1}$ | Temp. range/K | $\Delta(E/R)/\text{K}^c$ |
|---|--|--|-------------------------|---|---------------|--------------------------|
| <i>Peroxy radicals</i> | | | | | | |
| oFOx160 | $\text{CF}_3\text{C(O)O}_2 + \text{HO}_2 \rightarrow \text{CH}_3\text{C(O)OOH} + \text{O}_2$ | 1.8×10^{-12} | | | | |
| | $\rightarrow \text{CH}_3\text{C(O)OH} + \text{O}_3$ | 7.6×10^{-12} | | | | |
| | $\rightarrow \text{CH}_3\text{C(O)O} + \text{HO} + \text{O}_2$ | 1.12×10^{-11} | | | | |
| | Overall | 2.0×10^{-11} | 0.3 | | | |
| oFOx161 | $\text{CF}_3\text{C(O)O}_2 + \text{NO} \rightarrow \text{CF}_3\text{C(O)O} + \text{NO}_2$ | 2.8×10^{-11} | 0.2 | $4.0 \times 10^{-12} \exp(560/T)$ | 220–340 | 200 |
| oFOx162 | $\text{CF}_3\text{C(O)O}_2 + \text{NO}_2 + \text{M} \rightarrow \text{CF}_3\text{C(O)O}_2\text{NO}_2 + \text{M}$ | 6.6×10^{-12} | 0.3 | | | |
| oFOx163 | $\text{CF}_3\text{C(O)O}_2\text{NO}_2 + \text{M} \rightarrow \text{CF}_3\text{C(O)O}_2 + \text{NO}_2 + \text{M}$ | $7.95 \times 10^{-5} (1 \text{ bar})/s^{-1}$ | 0.3 | $5.0 \times 10^{-2} \exp(-12350/T) [\text{N}_2]$ | 290–330 | |
| | | $9.93 \times 10^{-5} (k_\infty/s^{-1})$ | | $1.1 \times 10^{17} \exp(-14440/T) (k_\infty/s^{-1})$ | | |
| <i>Photochemical reactions added to the IUPAC website (see Supplement for datasheets)</i> | | | | | | |
| PF5 | $\text{CHF}_2\text{CHO} + h\nu \rightarrow \text{products}$ | | | | | |
| PF6 | $\text{C}_2\text{F}_5\text{CHO} + h\nu \rightarrow \text{products}$ | | | | | |
| PF7 | $n\text{-C}_3\text{F}_7\text{CHO} + h\nu \rightarrow \text{products}$ | | | | | |
| PF8 | $n\text{-C}_4\text{F}_9\text{CHO} + h\nu \rightarrow \text{products}$ | | | | | |
| PF9 | $\text{CF}_3\text{CH}_2\text{CHO} + h\nu \rightarrow \text{products}$ | | | | | |
| PF10 | $n\text{-C}_6\text{F}_{13}\text{CH}_2\text{CHO} + h\nu \rightarrow \text{products}$ | | | | | |

^a Rate coefficients are also known as rate constants, both terms are used here. ^b See corresponding datasheets in Supplement for further information (e.g., methods used and products formed). ^c The cited uncertainty is an expanded uncertainty corresponding approximately to a 95% confidence limit.

in the Techniques and Comments sections are listed in Appendix A.

For measurements of relative rate coefficients, wherever possible the comments contain the actual measured ratio of rate coefficients together with the rate coefficient of the reference reaction used to calculate the absolute rate coefficient listed in the data table. The absolute value of the rate coefficient given in the table may be different from that reported by the original author owing to a different choice of rate coefficient of the reference reaction. Whenever possible the reference rate data are those preferred in the most recent IUPAC evaluation of that reaction.

The preferred values in the datasheets are based on our consideration of the suitability of experimental method and coverage of applicable parameter space (temperature, total pressure of diluent gas, partial pressure of gas-phase species) within the atmospherically relevant range. The general approach and methods used have been reviewed by Cox (2012). It is recognized that preferred values may change with publication of new data, and such changes are updated at the website. The preferred rate coefficients are presented (i) at a temperature of 298 K and (ii) in temperature dependent form over a stated temperature range. This is followed by a statement of the uncertainty limits in $\log k$ at 298 K and the uncertainty limits either in (E/R) or in n , (for systems with power law temperature dependence), for the mean temperature in the range. Some comments on the assignment of uncertainties are given later in this guide to the datasheets. The “Comments on Preferred Values” section describes how the selection was made and give any other relevant information. The extent of the comments depends upon the present state of our knowledge of the reaction in question. The datasheets are concluded with a list of the relevant references.

2.2 Conventions concerning rate coefficients

All of the reactions in the table are elementary processes. Thus the rate expression is derived from a statement of the reaction, e.g.



$$-\frac{1}{2} \frac{d[A]}{dt} = \frac{d[B]}{dt} = \frac{d[C]}{dt} = k[A]^2. \quad (1)$$

Note that the stoichiometric coefficient for A, i.e. 2, appears in the denominator before the rate of change of [A] (which is equal to $2k[A]^2$) and as a power on the right-hand side. Representations of k as a function of temperature characterize simple “direct” bimolecular reactions. Sometimes it is found that k also depends on the pressure and the nature of the bath gas. This may be an indication of complex-formation during the course of the bimolecular reaction, which is always the case in combination reactions. In the following sections the representations of k which are adopted in these cases are explained.

2.3 Treatment of combination and dissociation reactions

Unlike simple bimolecular reactions such as those considered in Sect. 2.2, combination reactions



and the reverse dissociation reactions



are composed of sequences of different types of physical and chemical elementary processes. Their rate coefficients reflect the more complicated sequential mechanism and depend on the temperature, T , and the nature and concentration of the third body, M . In this evaluation, the combination reactions are described by a formal second-order rate law:

$$\frac{d[AB]}{dt} = k[A][B] \quad (2)$$

while dissociation reactions are described by a formal first-order rate law:

$$-\frac{d[AB]}{dt} = k[AB]. \quad (3)$$

In both cases, k depends on the temperature and on the concentration of M , i.e., $[M]$. To rationalize the representations of the rate coefficients used in this evaluation, we first consider the Lindemann–Hinshelwood reaction scheme. The combination reactions follow an elementary mechanism of the form,



while the dissociation reactions are characterized by:



Assuming quasi-stationary concentrations for the highly excited unstable species AB^* (i.e. that $d[AB^*]/dt \approx 0$), it follows that the rate coefficient for the combination reaction is given by:

$$k = k_3 \left(\frac{k_4[M]}{k_{-3} + k_4[M]} \right) \quad (4)$$

while that for the dissociation reaction is given by:

$$k = k_{-4}[M] \left(\frac{k_{-3}}{k_{-3} + k_4[M]} \right) \quad (5)$$

In these equations the expressions before the parentheses represent the rate coefficients of the process initiating the reaction, whereas the expressions within the parentheses denote the fraction of reaction events which, after initiation,

complete the reaction to products. In the low pressure limit ($[M] \rightarrow 0$) the rate coefficients are proportional to $[M]$; in the high-pressure limit ($[M] \rightarrow \infty$) they are independent of $[M]$. It is useful to express k in terms of the limiting low pressure and high-pressure rate coefficients,

$$k_0 = \lim k([M]) \text{ for } [M] \rightarrow 0 \text{ and} \\ k_\infty = \lim k([M]) \text{ for } [M] \rightarrow \infty. \quad (6)$$

From this convention, the Lindemann–Hinshelwood equation is obtained

$$k = \frac{k_0 k_\infty}{k_0 + k_\infty}. \quad (7)$$

It follows that, for combination reactions, $k_0 = k_3 k_4 [M] / k_{-1}$ and $k_\infty = k_3$, while, for dissociation reactions, $k_0 = k_{-4} [M]$ and $k_\infty = k_{-3} k_{-4} / k_4$. Since detailed balancing applies, the ratio of the rate coefficients for combination and dissociation at a fixed T and $[M]$ is given by the equilibrium constant $K_c = k_3 k_4 / k_{-3} k_{-4}$.

Starting from the high-pressure limit, the rate coefficients fall off with decreasing third body concentration $[M]$ and the corresponding representation of k as a function of $[M]$ is termed the “falloff curve” of the reaction. In practice, the above Lindemann–Hinshelwood expressions do not suffice to characterize the falloff curves completely. Because of the multistep character of the collisional deactivation ($k_4 [M]$) and activation ($k_{-4} [M]$) processes, and energy- and angular momentum-dependences of the association (k_3) and dissociation (k_{-3}) steps, as well as other phenomena, the falloff expressions have to be modified. This can be done by including a broadening factor F to the Lindemann–Hinshelwood expression (Troe, 1979):

$$k = \frac{k_0 k_\infty}{k_0 + k_\infty} F = k_0 \left(\frac{1}{1+x} \right) F = k_\infty \left(\frac{x}{1+x} \right) F. \quad (8)$$

The broadening factor F depends on the ratio $x = k_0 / k_\infty$, which is proportional to $[M]$, and can be used as a measure of “reduced pressure”. The first factors on the right-hand side represent the Lindemann–Hinshelwood expression and the additional broadening factor F , at not too high temperatures, is approximately given by (Troe, 1979):

$$\log F \cong \frac{\log F_c}{1 + [\log(k_0/k_\infty)/N]^2} \quad (9)$$

where $\log = \log_{10}$ and $N \approx [0.75 - 1.27 \log F_c]$.

When F_c decreases, the falloff curve broadens and becomes asymmetric (i.e. $F(k_0/k_\infty) \neq F(k_\infty/k_0)$). The given equation for F then becomes insufficient and should be replaced, e.g. by

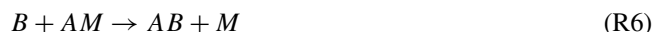
$$F(x) \approx (1+x)/(1+x^n)^{1/n} \quad (10)$$

where $x = k_0/k$, $n = [\ln 2 / \ln(2/F_c)][0.8 + 0.2x^q]$, $q = (F_c - 1) / \ln(F_c/10)$ and $\ln = \log_e$ (Troe and Ushakov, 2014). While

the former equation for $\log F$ appears acceptable as long as $F_c \geq 0.6$, the latter equation for F is more rigorous when $F_c \leq 0.6$. With these equations, falloff curves are represented in terms of the three parameters k_0 (being proportional to $[M]$), k_∞ , and F_c .

The parameters k_0 , k_∞ , and F_c depend on details of the intra- and intermolecular dynamics and in principle can be calculated. If the required information is not available, one has to obtain them by fitting experimental falloff curves with the expressions given above. Nevertheless, one may estimate F_c to be typically of the order of 0.49, 0.44, 0.39, and 0.35, if the reactants A and B in total have $r = 3, 4, 5$, and 6 external rotational degrees of freedom, respectively (Cobos and Troe, 2003; for the reaction $\text{HO} + \text{NO}_2 + M$, e.g. one would have $r = 5$ and $F_c \approx 0.39$); F_c may be lower, if low frequency vibrations in A or B are relevant in addition to the rotations and if collisions are inefficient. Over the range 200–300 K often one can neglect a temperature dependence of F_c (for detailed calculations of F_c , including a dependence on the bath gas M (see e.g. Troe, 1983; Troe and Ushakov, 2011, 2014). The accuracy of $F(x)$ as given above is estimated to be about 10 %. Larger differences between experimentally fitted F_c often are an indication for inadequate falloff extrapolations to k_0 and/or k_∞ . In this case, the apparent values for k_0 , k_∞ , and F_c still can provide a satisfactory representation of the considered experimental data, in spite of the fact that k_0 and/or k_∞ are not the real limiting values. If falloff curves are fitted in different ways, changes in F_c require changes in the limiting k_0 and k_∞ . In the present evaluation, we generally follow the experimentally fitted values for k_0 , k_∞ , and F_c , provided that F_c does not differ too much from the standard values given above and theoretically modelled values. If large deviations are encountered, the experimental data are re-evaluated using F_c -values as given above. One should also note that k_∞ for combination reactions without a barrier often have only weak temperature dependences which in many cases can be neglected.

Besides the energy-transfer mechanism, i.e., reactions (R3), (R-3), and (R4), a second mechanism may become relevant for some reactions considered here. This is the radical-complex (or chaperon) mechanism



which, in the low-pressure range, leads to $k_0 = (k_5/k_{-6})k_6[M]$. For some tri- and tetra-atomic adducts AB , e.g., $\text{O} + \text{O}_2 \rightarrow \text{O}_3$ and $\text{HO} + \text{C}_6\text{H}_6 \rightarrow \text{HOC}_6\text{H}_6$, the value of k_0 may exceed that from the energy-transfer mechanism and show stronger temperature dependences (Luther et al., 2005; Teplukhin and Babikov, 2016). This mechanism may also influence high-pressure experiments when k_0 from the radical-complex mechanism exceeds k_∞ from the energy-transfer mechanism (Oum et al., 2003). In this case

falloff over wide pressure ranges cannot be represented by contributions from the energy-transfer mechanism alone, in particular when measurements at pressures above about 10 bar are taken into consideration.

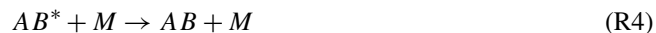
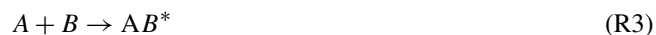
The dependence of k_0 and k_∞ on the temperature T is represented in the form $k \propto T^{-n}$ except for cases with an established energy barrier in the potential. We have used this form of temperature dependence because it usually gives a better fit to the data over a wider range of temperature than does the Arrhenius expression. It should be emphasised that the chosen form of the temperature dependence is often only adequate over limited temperature ranges such as 200–300 K. Obviously, the relevant values of n are different for k_0 and k_∞ . In this evaluation, values of k_0 are given for selected examples of third bodies M , and if possible for $M = \text{N}_2$, O_2 , or air.

2.4 Treatment of complex-forming bimolecular reactions

Bimolecular reactions may follow the “direct” pathway



and/or involve complex-formation, in the simplest way characterized by the steps



(there may be additional pathways following from AB^* ; direct and complex-forming pathways may or may not be coupled). Assuming quasi-stationary concentrations of AB^* (i.e. that $d[AB^*]/dt \approx 0$ as in Sect. 2.3), a Lindemann–Hinshelwood type analysis leads to

$$d[AB]/dt = k_{\text{Ass}}[A][B] \quad (11)$$

$$d[C]/dt = d[D]/dt = k_{\text{CA}}[A][B] \quad (12)$$

$$d[A]/dt = -(k_{\text{Ass}} + k_{\text{CA}})[A][B]. \quad (13)$$

The rate constants for association (k_{Ass}) and for chemical activation leading to product formation (k_{CA}) then are given by

$$k_{\text{Ass}} = k_1 k_2 [M] / (k_{-1} + k_2 [M] + k_5) \quad (14)$$

$$k_{\text{CA}} = k_1 k_5 / (k_{-1} + k_2 [M] + k_5). \quad (15)$$

Note that k_{Ass} and k_{CA} are dependent on the nature and concentration of the third body M , in addition to their temperature dependence. In reality, as for combination and dissociation reactions, the given expressions for k_{Ass} and k_{CA} have to be extended by suitable broadening factors F to account for the multistep character of processes (Reaction R4) and the energy- and angular momentum-dependences of processes (Reactions R3, R-3, and R8). These broadening factors, however, generally differ for k_{Ass} and k_{CA} ; also they generally

differ from those of simple combination reactions described in Sect. 2.3. One should note that association and chemical activation here are coupled such that their joint treatment is complicated. Some simplification is reached when the processes first are treated separately and the coupling is introduced at the end (Troe, 2015). The corresponding rate constants of the separated processes are denoted by k_{Ass}^* and k_{CA}^* and are given by

$$k_{\text{Ass}}^* = k_3 k_4 [M] / (k_{-3} + k_4 [M]) \quad (16)$$

and

$$k_{\text{CA}}^* = k_3 k_8 / (k_4 [M] + k_7). \quad (17)$$

k_{Ass}^* then corresponds to the rate constant of a combination reaction described in Sect. 2.3 and has a broadening factor $F_{\text{Ass}}^*(x^*)$. k_{CA}^* has to be treated in a different way and is expressed in the form

$$k_{\text{CA}}^* = k_{\text{Ass},\infty} [1 / (1 + x^*)] F_{\text{CA}}^*(x^*) \quad (18)$$

with $x^* = k_{\text{Ass},\infty} [M] / k_{\text{CA},\infty}^*$ and a broadening factor $F_{\text{CA}}^*(x)$ (Stewart et al., 1989). The latter factor is generally larger than $F_{\text{Ass}}^*(x^*)$ (Troe, 2015). The rate parameters $k_{\text{CA},0}^*$ and $k_{\text{CA},\infty}^*$ depend on the molecular parameters and can be calculated theoretically or fitted experimentally (after the coupling between association and chemical activation has been accounted for). In practice one may try to represent the rate constants in the form of rate constants of separated processes k_{Ass}^* and k_{CA}^* . Coupling these rate constants then leads to a full representation of the rate constants in terms of the six rate parameters $k_{\text{Ass},0}$, $k_{\text{Ass},\infty}$, $F_{\text{Ass},c}$, $k_{\text{CA},0}$, $k_{\text{CA},\infty}$, and $F_{\text{CA},c}$. If one neglects the coupling and fits these parameters directly from the experiments (Miller and Klippenstein, 2001), however, one has to be aware of the fact that the values obtained do not correspond to those of separated, single-channel, association and chemical activation processes (for more details, see Troe, 2015).

As a consequence of the multistep character of complex-forming bimolecular reactions, a variety of temperature – and pressure – dependences of k_{Ass} and k_{CA} are observed. The low-pressure limit of the total rate constants $k_{\text{tot}} = k_{\text{Ass}} + k_{\text{CA}}$, i.e., $k_{\text{tot},0} = k_{\text{CA},0} = k_3 k_8 / (k_{-3} + k_8)$, because of different energy – and angular momentum – dependences of the specific rate constants k_3 , k_{-3} , and k_7 , may increase or decrease with temperature, the latter with the possibility to a change with an increase above a certain temperature. k_{tot} , as given above, may increase with pressure from $k_{\text{CA},0}$ to k_1 , with $M = \text{H}_2\text{O}$ often being a particularly efficient third body in the pressure – dependent range. The pressure dependence generally becomes less apparent with increasing temperature. Finally, the further fate of an addition product AB is of importance. It may be collisionally reactivated to energies where $k_8 \gg k_{-3}$, such that formation of $C + D$ is enhanced (in comparison to energies where $k_8 \ll k_{-3}$). There is also

the possibility that $A - M$ (or $B - M$) complexes are formed which react in a chaperon mechanism with B (or A) and then form products. $M = \text{H}_2\text{O}$ here again may be particularly efficient. Without detailed theoretical analysis, in general, it will be difficult to disentangle the intrinsic mechanism. Therefore, reference to theoretical work is given for selected reactions.

2.5 Photochemical reactions

Tables are provided in the datasheets which summarise the available experimental data for: (i) absorption cross sections and (ii) quantum yields. These data are supplemented by a series of comments. The next table in each datasheet lists the preferred absorption cross section data and the preferred quantum yields at appropriate wavelength intervals. For absorption cross sections the intervals are usually 1, 5 or 10 nm. Any temperature dependence of the absorption cross sections is also given where possible. The aim in presenting these preferred data is to provide a basis for calculating atmospheric photolysis rates. For absorption continua the temperature dependence is often represented by Sulzer–Wieland type expressions (Astholz et al., 1981). Alternately a simple empirical expression of the form: $\log_{10}(\sigma_{T_1}/\sigma_{T_2}) = B^*(T_1 - T_2)$ is used. The comments again describe how the preferred data were selected and include other relevant points. The photochemical datasheets are concluded with a list of references.

2.6 Conventions concerning absorption cross sections

These are presented in the datasheets as “absorption cross sections per molecule, base e ”. They are defined according to the equation:

$$\sigma I/I_0 = \exp(-[N]I) \quad (19)$$

where I_0 and I are the transmitted light intensities in the absence and presence of absorber, $[N]$ is the number concentration of absorber (expressed in molec. cm^{-3}), l is the path length (expressed in cm), and σ is the absorption cross section (units of $\text{cm}^2 \text{ molec.}^{-1}$). Note that “molecule” is not a unit but is included here for clarity. Other definitions and units are frequently quoted. The closely related quantities “absorption coefficient” and “extinction coefficient” are often used, but care must be taken to avoid confusion in their definition, see Calvert (1990) for definitions and discussion. It is always necessary to know the units of concentration and of path length and the type of logarithm (base e or base 10) corresponding to the definition. The decadic molar absorption coefficient, ε , is often quoted, particularly in the older literature, and is defined as:

$$\varepsilon = \{1/([A]l)\} \log_{10}(I_0/I) \quad (20)$$

where $[A]$ is the concentration of the absorber expressed in units of moles per liter. While ε is often called an extinction coefficient, the term “extinction” should more properly

be used for the sum of absorption and scattering. To convert from ε (base 10, units of $\text{dm}^3 \text{ molec.}^{-1} \text{ cm}^{-1}$) to σ (base e , units of $\text{cm}^2 \text{ molec.}^{-1}$) multiply by 3.82×10^{-20} .

2.7 Assignment of uncertainties

Under the heading “reliability”, estimates have been made of the absolute accuracies of the preferred values of k at 298 K and of the preferred values of E/R over the quoted temperature range. The accuracy of the preferred rate coefficient at 298 K is quoted as the term $\Delta \log k$, where $\Delta \log k = d$ and d is defined by the equation, $\log k = c \pm d$. This is equivalent to the statement that k is uncertain to a factor of f , where $d = \log f$. The accuracy of the preferred value of E/R is quoted as the term $\Delta(E/R)$, where $\Delta(E/R) = g$ and g is defined by the equation $E/R = h \pm g$. d and g are uncertainties corresponding approximately to 95 % confidence limits. For second-order rate coefficients listed in this evaluation, an estimate of the uncertainty at any given temperature within the recommended temperature range may be obtained from the equation:

$$\Delta \log k(T) = \Delta \log k(298 \text{ K}) + 0.4343\{\Delta E/R(1/T - 1/298 \text{ K})\}. \quad (21)$$

The assignment of these absolute uncertainties in k and E/R is our subjective assessment. They are not determined by a rigorous, statistical analysis of the database, which is generally too limited to permit such an analysis. Rather, the uncertainties are based on our knowledge of the techniques, the difficulties of the experimental measurements, the potential for systematic errors, and the number of studies conducted and their agreement or lack thereof. Experience shows that for rate measurements of atomic and free radical reactions in the gas-phase, the precision of the measurement, i.e. the reproducibility, is usually good. Thus, for single studies of a particular reaction involving one technique, standard deviations, or even 95 % confidence limits, of $\pm 10\%$ or less are frequently reported in the literature. Unfortunately, when we compare data for the same reaction studied by more than one group of investigators and involving different techniques, the rate coefficients sometimes differ by a factor of 2 or even more. This can only mean that one or more of the studies has large systematic errors which are difficult to detect. This is hardly surprising since it is not always possible to study atomic and free radical reactions in isolation, and consequently mechanistic and other difficulties frequently arise. Our assessment of uncertainty limits tends towards the cautious side. Our assessment of uncertainties in the preferred values are not determined by a rigorous, statistical analysis of the database, which is generally too limited to permit such an analysis. Rather, the uncertainties are based on our knowledge of the techniques, the difficulties of the experimental measurements, the potential for systematic errors, and the number of studies conducted and their agreement or lack thereof.

Appendix A

Table A1. List of abbreviations.

| | |
|------|--|
| A | absorption |
| AS | absorption spectroscopy |
| CCD | charge coupled detector |
| CIMS | chemical ionization mass spectroscopy/spectrometry |
| CL | chemiluminescence |
| CRDS | cavity ring-down spectroscopy |
| DF | discharge flow |
| EPR | electron paramagnetic resonance |
| F | flow system |
| FP | flash photolysis |
| FTIR | Fourier transform infrared |
| FTS | Fourier transform spectroscopy |
| GC | gas chromatography/gas chromatographic |
| HPLC | high-performance liquid chromatography |
| IR | infrared |
| LIF | laser induced fluorescence |
| LMR | laser magnetic resonance |
| LP | laser photolysis |
| MM | molecular modulation |
| MS | mass spectrometry/mass spectrometric |
| P | steady state photolysis |
| PLP | pulsed laser photolysis |
| PR | pulse radiolysis |
| RA | resonance absorption |
| RF | resonance fluorescence |
| RR | relative rate |
| S | static system |
| TDLS | tunable diode laser spectroscopy |
| UV | ultraviolet |
| UVA | ultraviolet absorption |
| VUVA | vacuum ultraviolet absorption |

Code and data availability. No code was used; data were taken from the publications listed in the Supplement.

Supplement. The supplement related to this article is available online at <https://doi.org/10.5194/acp-26-6579-2026-supplement>.

Author contributions. All authors defined the scope of the work. TJW, JNC, and AM developed and drafted the datasheets and manuscript. All authors reviewed, refined, and revised the manuscript and datasheets.

Competing interests. At least one of the (co-)authors is a member of the editorial board of *Atmospheric Chemistry and Physics*. The peer-review process was guided by an independent editor, and the authors also have no other competing interests to declare.

Disclaimer. Publisher's note: Copernicus Publications remains neutral with regard to jurisdictional claims made in the text, published maps, institutional affiliations, or any other geographical representation in this paper. The authors bear the ultimate responsibility for providing appropriate place names. Views expressed in the text are those of the authors and do not necessarily reflect the views of the publisher.

Acknowledgements. The members of the Task Group wish to express their appreciation to IUPAC for the financial help which facilitated the preparation of this evaluation. Markus Ammann appreciates support by the Swiss National Science Foundation (grant no. 188662). We also acknowledge financial support from the Office Fédéral de l'Éducation et de la Science, the Centre National de la Recherche Scientifique-Institut National des Sciences de l'Univers (CNRS-INSU). Support was also obtained from the French Data Terra Research Infrastructure through the AERIS Atmosphere Data and Services Centre. We thank Cathy Boonne, Elliot Richard, and Maroua Soltani for developing and maintaining the website.

Financial support. This research has been supported by the Schweizerischer Nationalfonds zur Förderung der Wissenschaftlichen Forschung (grant no. 188662).

The article processing charges for this open-access publication were covered by the Max Planck Society.

Review statement. This paper was edited by Mingjin Tang and reviewed by four anonymous referees.

References

- Ammann, M., Cox, R. A., Crowley, J. N., Jenkin, M. E., Mellouki, A., Rossi, M. J., Troe, J., and Wallington, T. J.: Evaluated kinetic and photochemical data for atmospheric chemistry: Volume VI – heterogeneous reactions with liquid substrates, *Atmos. Chem. Phys.*, 13, 8045–8228, <https://doi.org/10.5194/acp-13-8045-2013>, 2013.
- Astholz, D. C., Brouwer, L., and Troe, J.: High-temperature ultraviolet-absorption spectra of polyatomic molecules in shock waves, *Ber. Bunsenges. Phys. Chem.*, 85, 559–564, <https://doi.org/10.1002/bbpc.19810850708>, 1981.
- Atkinson, R., Baulch, D. L., Cox, R. A., Hampson Jr., R. F., Kerr, J. A., and Troe, J.: Evaluated kinetic and photochemical data for atmospheric chemistry: Supplement III, IUPAC Subcommittee on Gas Kinetic Data Evaluation for Atmospheric Chemistry, *J. Phys. Chem. Ref. Data*, 18, 881–1097, <https://doi.org/10.1063/1.555832>, 1989.
- Atkinson, R., Baulch, D. L., Cox, R. A., Hampson Jr., R. F., Kerr, J. A., and Troe, J.: Evaluated kinetic and photochemical data for atmospheric chemistry: Supplement IV, IUPAC Subcommittee on Gas Kinetic Data Evaluation for Atmospheric Chemistry, *J. Phys. Chem. Ref. Data*, 21, 1125–1568, <https://doi.org/10.1063/1.555918>, 1992.

- Atkinson, R., Baulch, D. L., Cox, R. A., Hampson Jr., R. F., Kerr, J. A., Rossi, M., and Troe, J.: Evaluated kinetic, photochemical, and heterogeneous data for atmospheric chemistry: Supplement V, IUPAC Subcommittee on Gas Kinetic Data Evaluation for Atmospheric Chemistry, *J. Phys. Chem. Ref. Data*, 26, 521–1011, <https://doi.org/10.1063/1.556011>, 1997a.
- Atkinson, R., Baulch, D. L., Cox, R. A., Hampson Jr., R. F., Kerr, J. A., Rossi, M. J., and Troe, J.: Evaluated kinetic and photochemical data for atmospheric chemistry: Supplement VI, IUPAC Subcommittee on Gas Kinetic Data Evaluation for Atmospheric Chemistry, *J. Phys. Chem. Ref. Data*, 26, 1329–1499, <https://doi.org/10.1063/1.556010>, 1997b.
- Atkinson, R., Baulch, D. L., Cox, R. A., Hampson Jr., R. F., Kerr, J. A., Rossi, M. J., and Troe, J.: Evaluated kinetic and photochemical data for atmospheric chemistry: Supplement VII, IUPAC Subcommittee on Gas Kinetic Data Evaluation for Atmospheric Chemistry, *J. Phys. Chem. Ref. Data*, 28, 191–393, <https://doi.org/10.1063/1.556048>, 1999.
- Atkinson, R., Baulch, D. L., Cox, R. A., Hampson Jr., R. F., Kerr, J. A., Rossi, M. J., and Troe, J.: Evaluated kinetic and photochemical data for atmospheric chemistry, Supplement VIII, IUPAC Subcommittee on Gas Kinetic Data Evaluation for Atmospheric Chemistry, *J. Phys. Chem. Ref. Data*, 29, 167–266, <https://doi.org/10.1063/1.556058>, 2000.
- Atkinson, R., Baulch, D. L., Cox, R. A., Crowley, J. N., Hampson, R. F., Hynes, R. G., Jenkin, M. E., Rossi, M. J., and Troe, J.: Evaluated kinetic and photochemical data for atmospheric chemistry: Volume I – gas phase reactions of O_x , HO_x , NO_x , and SO_x species, *Atmos. Chem. Phys.*, 4, 1461–1738, <https://doi.org/10.5194/acp-4-1461-2004>, 2004.
- Atkinson, R., Baulch, D. L., Cox, R. A., Crowley, J. N., Hampson, R. F., Hynes, R. G., Jenkin, M. E., Rossi, M. J., and Troe, J.: Evaluated kinetic and photochemical data for atmospheric chemistry: Volume II – gas phase reactions of organic species, *Atmos. Chem. Phys.*, 6, 3625–4055, <https://doi.org/10.5194/acp-6-3625-2006>, 2006.
- Atkinson, R., Baulch, D. L., Cox, R. A., Crowley, J. N., Hampson, R. F., Hynes, R. G., Jenkin, M. E., Rossi, M. J., and Troe, J.: Evaluated kinetic and photochemical data for atmospheric chemistry: Volume III – gas phase reactions of inorganic halogens, *Atmos. Chem. Phys.*, 7, 981–1191, <https://doi.org/10.5194/acp-7-981-2007>, 2007.
- Atkinson, R., Baulch, D. L., Cox, R. A., Crowley, J. N., Hampson, R. F., Hynes, R. G., Jenkin, M. E., Rossi, M. J., Troe, J., and Wallington, T. J.: Evaluated kinetic and photochemical data for atmospheric chemistry: Volume IV – gas phase reactions of organic halogen species, *Atmos. Chem. Phys.*, 8, 4141–4496, <https://doi.org/10.5194/acp-8-4141-2008>, 2008.
- Baulch, D. L., Cox, R. A., Hampson Jr., R. F., Kerr, J. A., Troe, J., and Watson, R. T.: Evaluated kinetic and photochemical data for atmospheric chemistry, CODATA Task Group on Chemical Kinetics, *J. Phys. Chem. Ref. Data*, 9, 295–471, <https://doi.org/10.1063/1.555619>, 1980.
- Baulch, D. L., Cox, R. A., Crutzen, P. J., Hampson Jr., R. F., Kerr, J. A., Troe, J., and Watson, R. T.: Evaluated kinetic and photochemical data for atmospheric chemistry: Supplement I, CODATA Task Group on Chemical Kinetics, *J. Phys. Chem. Ref. Data*, 11, 327–496, <https://doi.org/10.1063/1.555664>, 1982.
- Baulch, D. L., Cox, R. A., Hampson Jr., R. F., Kerr, J. A., Troe, J., and Watson, R. T.: Evaluated kinetic and photochemical data for atmospheric chemistry: Supplement II, CODATA Task Group on Gas Phase Chemical Kinetics, *J. Phys. Chem. Ref. Data*, 13, 1259–1380, <https://doi.org/10.1063/1.555721>, 1984.
- Brown, J. S.: HFOs: new, low global warming potential refrigerants, *ASHRAE J.*, 51, 22–29, 2009.
- Burkholder, J. B., Cox, R. A., and Ravishankara, A. R.: Atmospheric degradation of ozone depleting substances, their substitutes, and related species, *Chem. Rev.*, 115, 3704–3759, <https://doi.org/10.1021/cr5006759>, 2015.
- Calvert, J. G.: Glossary of atmospheric chemistry terms, *Pure Appl. Chem.*, 62, 2167–2219, <https://doi.org/10.1351/pac199062112167>, 1990.
- Cobos, C. J. and Troe, J.: Prediction of reduced falloff curves for recombination reactions at low temperatures, *Z. Phys. Chem.*, 217, 1–14, <https://doi.org/10.1524/zpch.217.8.1031.20428>, 2003.
- Cox, R. A.: Evaluation of laboratory kinetics and photochemical data for atmospheric chemistry applications, *Chem. Soc. Rev.*, 41, 6231–6246, <https://doi.org/10.1039/c2cs35092k>, 2012.
- Cox, R. A., Ammann, M., Crowley, J. N., Herrmann, H., Jenkin, M. E., McNeill, V. F., Mellouki, A., Rossi, M. J., Troe, J., and Wallington, T. J.: IUPAC in the (real) clouds: 40 years of evaluating atmospheric chemistry data, *Chem. Int.*, 40, 52, <https://doi.org/10.1515/ci-2018-0404>, 2018.
- Cox, R. A., Ammann, M., Crowley, J. N., Herrmann, H., Jenkin, M. E., McNeill, V. F., Mellouki, A., Rossi, M. J., Troe, J., and Wallington, T. J.: Evaluated kinetic and photochemical data for atmospheric chemistry: Volume VII – Criegee intermediates, *Atmos. Chem. Phys.*, 20, 13497–13519, <https://doi.org/10.5194/acp-20-13497-2020>, 2020.
- Crowley, J. N., Ammann, M., Cox, R. A., Hynes, R. G., Jenkin, M. E., Mellouki, A., Rossi, M. J., Troe, J., and Wallington, T. J.: Evaluated kinetic and photochemical data for atmospheric chemistry: Volume V – heterogeneous reactions on solid substrates, *Atmos. Chem. Phys.*, 10, 9059–9223, <https://doi.org/10.5194/acp-10-9059-2010>, 2010.
- Ellis, D. A., Martin, J. W., De Silva, A. O., Mabury, S. A., Hurley, M. D., Sulbaek Andersen, M. P., and Wallington, T. J.: Degradation of fluorotelomer alcohols: A likely atmospheric source of perfluorinated carboxylic acids, *Environ. Sci. Tech.*, 38, 3316–3321, <https://doi.org/10.1021/es049860w>, 2004.
- Giesy, J. P. and Kannan, K.: Global distribution of perfluorooctane sulfonate in wildlife, *Environ. Sci. Technol.*, 35, 1339–1342, <https://doi.org/10.1021/es001834k>, 2001.
- Lau, C., Anitole, K., Hodes, C., Lai, D., Pfahles-Hutchens, A., and Seed, J.: Perfluoroalkyl acids: A review of monitoring and toxicological findings, *Toxicol. Sci.*, 99, 366–394, <https://doi.org/10.1093/toxsci/kfm128>, 2007.
- Luther, K., Oum, K. and Troe, J.: The role of the radical-complex mechanism in the ozone recombination/dissociation reaction, *Phys. Chem. Chem. Phys.*, 7, 2764–2770, <https://doi.org/10.1039/b504178c>, 2005.
- Mellouki, A., Ammann, M., Cox, R. A., Crowley, J. N., Herrmann, H., Jenkin, M. E., McNeill, V. F., Troe, J., and Wallington, T. J.: Evaluated kinetic and photochemical data for atmospheric chemistry: Volume VIII – gas phase reactions of organic species with four, or more, carbon atoms ($\geq C_4$), *Atmos. Chem. Phys.*, 21, 4797–4808, <https://doi.org/10.5194/acp-21-4797-2021>, 2021.

- Miller, J. and Klippenstein, S. J.: The reaction between ethyl and molecular oxygen: Further analysis, *Int. J. Chem. Kinet.* 33, 654–668, <https://doi.org/10.1002/kin.1063>, 2001.
- Oum, K., Sekiguchi, K., Luther, K., and Troe, J.: Observation of unique pressure effects in the combination reaction of benzyl radicals in the gas to liquid transition region, *Phys. Chem. Chem. Phys.*, 5, 2931–2933, <https://doi.org/10.1039/b305954e>, 2003.
- Prevedouros, C., Cousins, I. T., Buck, R. C., and Korzeniowski, S. H.: Sources, fate and transport of perfluorocarboxylates, *Environ. Sci. Technol.*, 40, 32–44, <https://doi.org/10.1021/es0512475>, 2006.
- Stewart, P. H., Larson, C. W., and Golden, D. M.: Pressure and temperature dependence of reactions proceeding via a bound complex. 2. An application to $2\text{CH}_3 \rightarrow \text{C}_2\text{H}_5 + \text{H}$, *Combust. Flame*, 75, 25–31, [https://doi.org/10.1016/0010-2180\(89\)90084-9](https://doi.org/10.1016/0010-2180(89)90084-9), 1989.
- Teplukhin, A. and Babikov, D.: A full-dimensional model of ozone forming reaction: the absolute value of the recombination rate coefficient, its pressure and temperature dependencies, *Phys. Chem. Chem. Phys.*, 18, 19194–19206, <https://doi.org/10.1039/c6cp02224c>, 2016.
- Troe, J.: Theory of thermal unimolecular reactions in the fall-off range. I. Strong collision rate constants, *Ber. Bunsenges. Phys. Chem.*, 87, 161–169, <https://doi.org/10.1002/bbpc.19830870217>, 1983.
- Troe, J.: Predictive possibilities of unimolecular rate theory, *J. Phys. Chem.*, 83, 114–126, <https://doi.org/10.1021/j100464a019>, 1979.
- Troe, J.: Simplified representation of partial and total rate constants of complex-forming bimolecular reactions, *J. Phys. Chem. A*, 119, 12159–12165, <https://doi.org/10.1021/acs.jpca.5b06019>, 2015.
- Troe, J. and Ushakov, V. G.: Revisiting falloff curves of thermal unimolecular reactions, *J. Chem. Phys.*, 135, 054304, <https://doi.org/10.1063/1.3615542>, 2011.
- Troe, J. and Ushakov, V. G.: Representation of “Broad” Falloff Curves for Dissociation and Recombination Reactions, *Z. Phys. Chem.*, 228, 1–10, <https://doi.org/10.1515/zpch-2014-0468>, 2014.
- Velders, G. J. M., Fahey, D. W., Daniel, J. S., McFarland, M., and Andersen, S. O.: The large contribution of projected HFC emissions to future climate forcing, *P. Natl. Acad. Sci. USA*, 106, 10949–10954, <https://doi.org/10.1073/pnas.0902817106>, 2009.
- Wallington, T. J., Sulbaek Andersen, M. P., and Nielsen, O. J.: Atmospheric chemistry of short-chain haloolefins: Photochemical ozone creation potentials (POCPs), global warming potentials (GWPs), and ozone depletion potentials (ODPs), *Chemosphere*, 129, 135–141, <https://doi.org/10.1016/j.chemosphere.2014.06.092>, 2015.
- Wallington, T. J., Sulbaek Andersen, M. P., and Nielsen, O. J.: Atmospheric Chemistry of Halogenated Organic Compounds, in: *Advances in Atmospheric Chemistry*, edited by: Barker, J. R., Steiner, A., and Wallington, T. J., World Scientific, https://doi.org/10.1142/9789813147355_0005, 2017.